Automotive Science and Engineering, Vol. 11, No. 2, (2021), 3547-3559

Iran University of Science and Technology

Automotive Science and Engineering

Journal Homepage: ase.iust.ac.ir

ISSN: 2717-2023

Modeling and Optimization of Diesel-Natural Gas RCCI Engine Performance, Combustion Noise and Emissions using Response Surface Method

Behzad Borjian Fard[1], Bahram Bahri[1*], Ayat Gharehghani[2]

[1]Automotive, Fuel and Emission Research Center (AFERC), Department of Automotive Engineering, Shahreza Branch, Islamic Azad University, Shahreza, Iran
[2]School of Mechanical Engineering, Iran University Science and Technology, Narmak, Tehran 16844, Iran

ARTICLE INFO

Article history:
Received : 20 Feb 2020
Accepted:28 Aug 2020
Published:1 June 2021

Keywords:
RCCI
Emission
Combustion noise level
Response surface Method

A B S T R A C T

Reactivity control compression ignition (RCCI) engines have demonstrated high-efficient and clean combustion but still suffer from ringing operation at upper load and production of unburned hydrocarbon (uHC) and carbon monoxide (CO) emissions at lower load. In this study, statistical analysis and experimental testing were conducted to consider the effects of input parameters such as intake temperature (Tin), equivalent ratio (Φ) and engine speed on emissions, combustion noise and performance of a 0.5 liter RCCI engine using response surface method (RSM) with the aim to minimize emissions and combustion noise and to maximize parameters of performance. The developed models for measured responses like uHC, CO, nitrogen oxides (NOx) and calculated responses such as indicated mean effective pressure (IMEP) and combustion noise level (CNL) were statistically considered to be significant by analysis of variance (ANOVA). Interactive effects between T_{in}, Φ and engine speed for all operating points were analyzed by 3-D response surface plots. The results from this study indicated that at optimum input parameters, the values of uHC, CO, NOx, IMEP and CNL were found to be 90.3 (ppm), 106.8 (ppm), 248.2 (ppm), 11.7 (bar) and 87 (db), respectively. The models were validated by confirmatory tests, indicating the error in prediction less than 5%.

*Corresponding Author Tel.: +98 917 7124248; Fax: +98 31 53292064.
Email address: bahri@iaush.ac.ir (Bahram Bahri)
https://doi.org/10.22068/ase.2020.533

[DOI: 10.22068/ase.2020.533]

1. Introduction

The demand for reduction of greenhouse gases and the introduction of stringent governmental regulations around the world have urged scientists and engine makers to increase efficiency from the internal combustion engine (ICE) by using alternative technologies [1-5]. Reactivity control compression ignition (RCCI) is a promising method among low temperature combustion (LTC) concepts to achieve clean combustion due to lower production of engine-out particulate matter (PM) and nitrogen oxides (NOx) emissions, while performing more thermal efficiency than conventional diesel combustion (CDC) [6-8].

In the dual fuel RCCI approach, least two separate fuels with different reactivity, a high-cetane fuel with good auto-ignition properties such as bio-diesel or diesel and a high reactivity fuel which have less reactive characteristics like gasoline or natural gas (NG) affects on the injection. Firstly, low reactivity fuel is injected in the intake port and then after interring the well-mixed charge into the cylinder and during the end of compression stroke (around piston top dead center (TDC), a low reactivity fuel injected directly into the cylinder and combustion chamber while the temperature of mixture becomes extremely enough [9,10]. So, the ignition can starts using single or multiple injections, from the higher concentrations regions of more reactive fuel and then spreads into the other regions of the combustion chamber. Combustion phasing characteristics could be determined by the two fuels mixing ratio, parameters of injection and in-cylinder reactivity gradient [11,12].

Compared to conventional compression ignition (CI) engines, high carbon monoxide (CO) and unburned hydrocarbon (uHC) emissions levels at low load (lower zone) operating region and ringing phenomenon at upper zone of RCCI operation (high loads) are some major limitations of RCCI [10]. Also, RCCI engine operation is constrained by combustion noise and high levels of peak pressure rise rate (PPRR) at high loads and losses of combustion efficiencies at low load [11]. Thus, finding RCCI engine operating regions which have moderate and lower CO, uHC and noise between low and high loads is desirable.

This paper aims to explore the operating regions of RCCI engine with lower emissions, combustion noise and higher performance using response surface methodology (RSM). RSM is a technique that contains collection of statistical and mathematical methods that are beneficial for problems analysis and data driven modeling and optimization [13, 14].

In several earlier works, RSM has been popularly used for modeling and optimizing exhaust emissions and engine parameters [13-25] which are listed in Figure 1. Depending on the type of ICE, these studies can be categorized into three main groups. The first group includes using RSM to optimize performance parameters [15, 16, 17, 18], improve engine performance and exhaust emission characteristics [13,14,19,20] and optimization of engine parameters to reduce noise [21] in CI engines. The second group includes using RSM for SI engines to optimize of performance and exhaust emission parameters [22-24]. The third group belongs to application of RSM for optimizing RCCI engine exhaust emissions [25].

In this part, some of the important and recent works are explained in detail. The ratios of n-butanol and cotton oil in diesel fuel were investigated by Atmanli et al. [14] using RSM for improving exhaust emissions and engine performance of direct injection CI engine. It was shown that CO, NOx and HC emissions dramatically decreased by using the optimum blend of three fuels when brake specific fuel consumption (BSFC) increased compared to those of diesel fuel but brake mean effective pressure (BMEP), brake power (BP) and brake torque (BT) decreased. Rajesh Kumar et al. [19] utilized advanced biofuel/diesel blends in CI engine to analyze the effects of exhaust gas recirculation and injection-timing on emissions and performance using developed mathematical models in RSM in which modeled and optimized the measured responses like PM, NOx and brake specific fuel consumption that are affected by input factors by multiple regression using RSM. Saravanan et al. [20] used RSM to

[DOI: 10.22068/ase.2020.533]

model all responses like brake thermal efficiency (BTE), NOx, PM and BSFC to improve CI engine exhaust emission. The objective of this work was to minimize NOx and PM emissions simultaneously with maximum BTE and minimum BSFC.

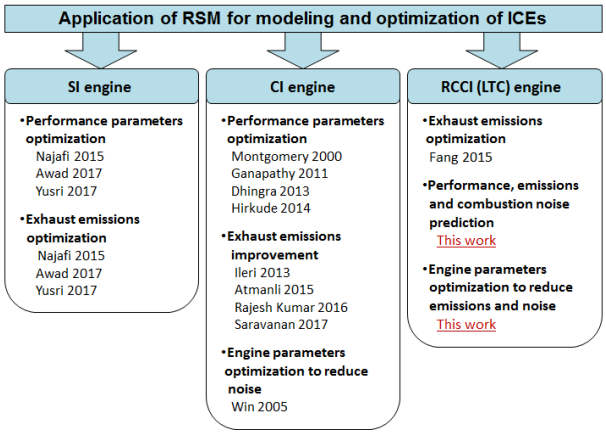

Figure 1: Prior studies including application of RSM for modeling and optimization of ICEs.

In a study conducted by Najafi et al. [22], an SI engine which operates with gasoline-ethanol blends of 5%, 7.5%, 10%, 12.5% and 15% was used with the aim to maximize SI performance parameters and minimizing exhaust emissions by using RSM. Awad et al. [23] used the multi-objective optimization to maximize the BP, BTE and minimize the NOx, HC, CO and BSFC emissions. A gasoline-butanol SI engine was used by Yusri et al. [24] to optimize blending ratio by RSM under different speeds of engine. They stated that the gasoline-butanol optimum mixing ratio regarding the emission and performance of SI engine was with 85% gasoline and 15% butanol. Fang et al. [25] employed RSM to optimize exhaust emission in RCCI engine.

In this paper, RSM is utilized to predict and model the responses. The contributions of this paper are as follows: (i) To explore the main and individual effects of intake temperature (T_{in}), equivalent ratio (Φ) and engine speed (N) on engine performance, combustion noise level (CNL) and emission characteristics. (ii) To develop experimental data driven regression models for predicting uHC, CO, NOx, indicated mean effective pressure (IMEP) and CNL for all experimental data. (iii) Determination of an optimum combination of the considered input factors by using RSM to minimize uHC, CO and NOx. The structure of the paper is as follows. Section 2 explains the engine experimental methodology and describes the operating conditions of the data points used in this study. The effect of RCCI engine operation on engine parameters and combustion noise is investigated in Section 3 by using RSM. Section 4 presents the summary and conclusions of this paper.

2. Experimental methodology

The single-cylinder variable compression ratio (VCR) Ricardo E6 diesel engine was converted to RCCI engine for the current study. Table 1 lists the major engine specifications for Ricardo engine.

Table 1: Ricardo E6/MS engine specifications.

Parameters (unit)	Value
Number of cylinders (-)	1
Compression ratio (-)	17.2
Bore (mm)	76.2
Stroke (mm)	110
Displacement volume (lit)	0.507
Number of valves	2
Intake valve opening (CAD bTDC)	7
Intake valve closing (CAD aBDC)	36
Exhaust valve opening (CAD bBDC)	36
Exhaust valve closing (CAD aTDC)	7

2.1. Experimental setup

Figure 2 shows the schematic figure of RCCI experimental setup and used measuring devices. Tested engine is a 0.507 liter sing-cylinder diesel engine which was manufactured by Ricardo company and has been modified to run in RCCI mode operation. Bore and stroke of tested engine are 76 and 111 mm, respectively and its compression ratio is set on 17 during the experimental tests. Low reactivity fuel (i.e. natural gas) is fed throughout the intake

[DOI: 10.22068/ase.2020.533]

manifold while the high reactivity fuel (i.e. diesel oil) is supplied directly to the cylinder. To regulate the engine speed and torque, one 22 KW electric dynamometer was used. To measure the in-cylinder pressure, an AVL QC43D water cooled, piezo-electric type pressure transducer was applied. A magnetic rotary encoder (i.e. Fotek MES-2,500D-T) was coupled to the crankshaft and measured the crank angle degree with the resolution of 2500 pulses per revolution (PPR). An air heater which was set up in the intake manifold was used to adjust the intake charge temperature. To provide the natural gas fuel, a high-pressure CNG reservoir was utilized and a gas regulator has been kept constant the pressure of CNG reservoir.

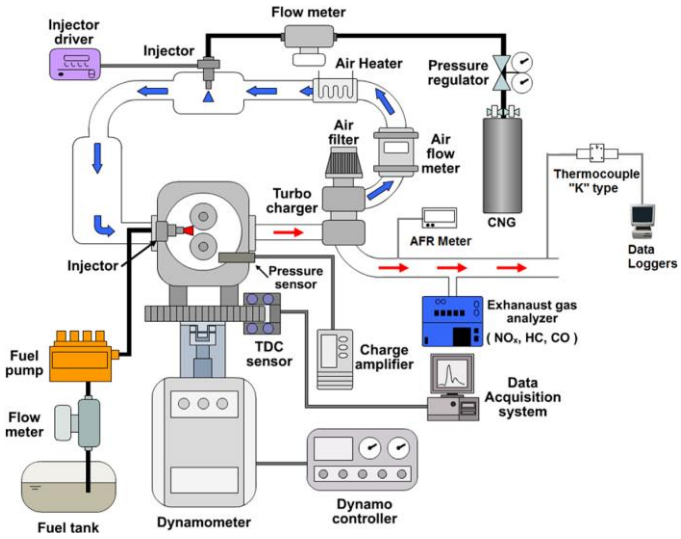

Figure 2: Schematic of the experimental setup used for collecting RCCI data for Ricardo engine [6].

A YAMATAKE flow meter was used to calculate the mass flow rate of CNG fuel and an air fuel ratio (AFR) indicator system was mounted on the exhaust manifold to sense the AFR of the intake charge. The intake charge and exhaust gas temperatures were measured by using a K-type thermocouple with an accuracy of ±1◦C. An AVL-735 fuel meter which contains the fuel conditioner devices was applied to calculate the diesel fuel mass flow rate during the experiments.

Table 2: Experimental uncertainty values.

Parameters (unit)	Uncertainty (%)
Temperature (◦C)	< 2
Pressure (bar)	< 2
Engine speed (rpm)	< 1
Fuel flow rate (kg/h)	< 1
Air flow rate (m3/h)	< 1

A three-hole injector nozzle that operates with pressure of 150 to 200 bars and the diameter of its holes is 0.25 mm, was used to inject the liquid fuel into the cylinder. Table 2 presents the values of uncertainty for experimental data. During the experiments, the in-cylinder pressure of 200 successive cycles were gathered and evaluated to show the characteristics of each RCCI operating point. The uncertainty values for experimental data are presented in Table 2.

2.2. Combustion noise level (CNL)

Three main in-cylinder pressure-based metrics such as PPRR, ringing intensity (RI) and CNL have been previously utilized to identify ringing operation of LTC engines [26- 27]. In this study, CNL is used to calculate RCCI engine noise level. CNL algorithm developed in [26] uses in-cylinder pressure trace to calculate CNL. The CNL calculation process is shown in Figure 3 by the following steps:

Step1: Applying a fast Fourier transform (FFT) for converted in-cylinder gas pressure P(t) from time to the frequency domain P(ω),

Step2: Simulate the noise attenuation by applying filters [26] for P(ω) and acquire filtered pressure (P_{filt}),

Step3: Calculate root mean square (RMS) value of the P_{filt} (P_{RMS}),

Step4: Calculate CNL in dB by comparing PRMS to a reference sound level [26].

[DOI: 10.22068/ase.2020.533]

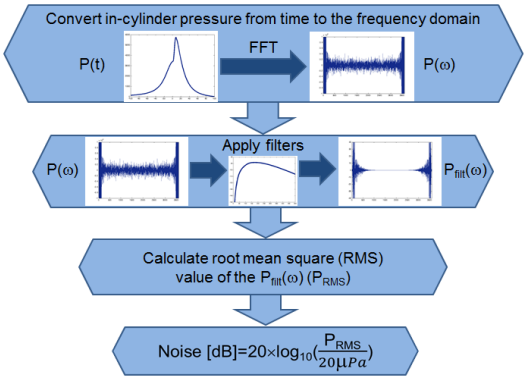

Figure 3: Schematic of the CNL algorithm [26] used in this study.

2.3. Experimental design

The factors studied in this paper with their chosen levels are shown in Table 3. For design of experiments, T_{in}, Φ and engine speed were considered as factors. Among these factors, T_{in} and Φ is considered as numeric variables in three levels with discrete values but engine speed is treated as a categoric factor in two levels. The five response variables were uHC, CO, NOx, IMEP and CNL.

Table 3: Experimental range and levels.

Variables	Unit	Type	Low level	High level
A: Equivalent ratio (Φ)	[-]	Numeric	0.3	0.4
B: Intake temperature (T_{in})	[◦C]	Numeric	150	190
C: Engine speed (N)	[rpm]	Categoric	800	1500

Table 3 presents experimental design matrix and the low and high levels of each variable as well as the results obtained for each designed experiment. This data is used to investigate the effect of RCCI operating parameters on uHC, CO, NOx, IMEP and CNL variation by regression modeling, second order polynomial models and graphical analysis.

RSM is a collection of mathematical and statistical techniques that are useful for modeling and analysing problems in which the objective is to optimize a response that is influenced by several factors. In Figure 4 is presented a schematic of implementation procedure by using RSM. As shown, after experimental design and after conducting the experiments to evaluate the influence of the independent variables on the responses obtained, second degree polynomial empirical models were developed by Eq. (1) [6]:

$$Y = \beta_0 + \sum_{i=1}^{k} \beta_i X_i + \sum_{i=1}^{k} \beta_{ii} X_i^2 + \sum_{i=1}^{k} \sum_{j=1}^{k} \beta_{ij} X_i X_j + \varepsilon \quad (1)$$

where Y is the response (predicted), Xi and Xj are numeric values and coded levels of the input factors, terms β_0, β_i, β_{ii} and β_{ij} are regression coefficients, i and j are linear and quadratic coefficients, k is the number of patterns and " is the experimental error.

This study adopts a central composite design (CCD) and RSM to evaluate the effect of RCCI engine operational factors on responses and to optimize the Equation numbers, within parentheses, are to position flush right, as in most effective variables on responses. 26 experiments were designed and the obtained RCCI engine experimental data at steady-state operating conditions which were analyzed using Design Expert (dx-7) software trial version.

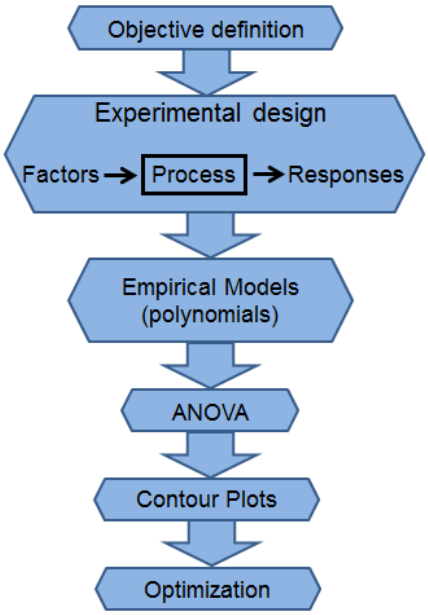

Figure 4: Schematic of the response surface methodology.

2.4. Central composite design

[DOI: 10.22068/ase.2020.533]

A widely used experimental design method in process optimization studies, known as CCD, has been used in this study to establish a second-order response surface model. One of the main benefits of using CCD as an effective alternative to full factorial design is that it enables more data to be gathered using fewer experiments. What distinguishes CCD from other methods is the use of axial points as defined values. Two or more experiments are required to be conducted for each parameter, which are at the lowest and highest levels. As mentioned earlier, the quadratic effect can be defined more precisely experimenting with each factor at 5 levels. The use of different values is dependent on the rotatability and orthogonality of the design and number of experiments.

2.5. Analysis of variance

In this study, analysis of variance (ANOVA) is used to investigate statistically the relationship between a response variable and factors. As shown in Figure 4, ANOVA was also utilized to validate the quality of RSM developed models for all the responses (uHC, CO, NOx, IMEP and CNL). For each response, the results were analyzed with the software using a quadratic model. Identification of the most significant factors is also described by ANOVA. For each model, p-values less than 0.05 present that the effect of model factors are significant within the 95% confidence level. The ability of the quadratic polynomial empirical to predict responses and the fitting quality were articulated on the basis of regression statistics goodness of fit (R^2) and adjusted R^2.

3. Results and discussion

3.1. Model analysis and evaluation

To optimize the independent variables, a CCD response surface methodology was used. The significance levels (p values) obtained by ANOVA for each model term is presented in Table 4 for the factors and their interactions.

As shown in Table 4, all models are significant as p-values are less than 0.05. The R^2 and adjusted R^2 for each model are presented in Table 5. An amount of R^2 near 1 for each model implies an excellent agreement between the experimental and predicted data. uHC, CO, NOx and CNL have meaningful fitness between the experimental and predicted values with R^2, 0.9213, 0.9752, 0.9186 and 0.9584, respectively.

Table 4: p-values for model terms of ANOVA analysis for each response.

Sourse	uHC	CO	NOx	IMEP	CNL
Model	< 0.0001	< 0.0001	< 0.0001	< 0.0001	< 0.0001
A	< 0.0008	< 0.0014	< 0.0001	0.1855	0.0526
B	< 0.0001	< 0.0001	< 0.0001	< 0.0001	< 0.0001
C	0.1358	0.0361	0.0126	< 0.0001	< 0.0001
AB	< 0.0041	0.0002	0.0002	0.6943	0.4265
AC	0.8486	0.6040	0.3501	0.0699	0.0277
BC	0.6215	0.2900	0.2505	0.2386	0.0233
A^2	0.5919	0.5665	0.5189	0.5212	0.4479
B^2	0.0999	< 0.0001	0.0338	0.5237	0.6737

Table 5: R^2 and Adj R^2 comparison between predicted and experimental.

Model	uHC	CO	NOx	IMEP	CNL
R^2	0.9213	0.9752	0.9186	0.8313	0.9584
Adj R^2	0.8988	0.9636	0.8803	0.7520	0.9338

3.2. uHC emissions

As shown in Table 4, Φ (factor A) and T_{in} (factor B) and their interaction have significant effect on uHC but engine speed (factor) C and all the square terms (A2 and B2) were not found to have significant influence Figure 5 shows the interaction effect of Φ and T_{in} on uHC with different engine speed (800 and 1500 rpm). Since minimum amount of uHC is desirable, for both figures shown in Figure 5, increasing Φ and T_{in} can decrease the amount of uHC due to high combustion temperature.

[DOI: 10.22068/ase.2020.533]

Also, lower amount of uHC can be occurred where the Φ and T_{in} are high. In addition, better results for uHC amount were obtained for the RCCI experimental data at 1500 rpm. ANOVA has already shown that the model of predicted uHC emission is significant. As previously mentioned, the amount of uHC emission is higher for the RCCI mode than CDC.

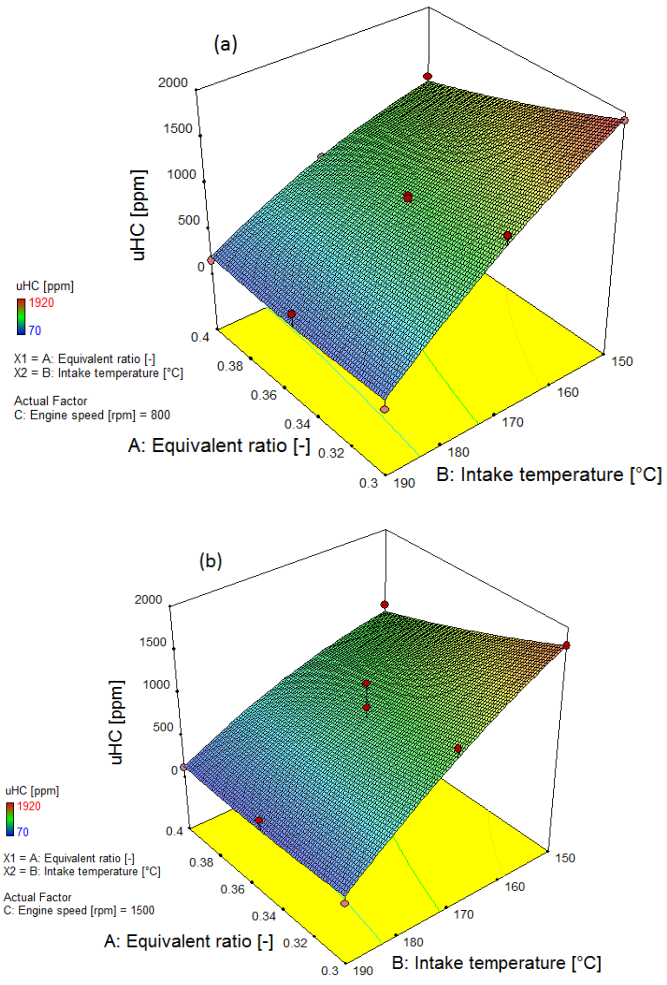

Figure 5: The interaction effects of Φ and T_{in} on uHC emissions for two levels of engine speeds (a) 800 rpm and b) 1500 rpm)

Replacing the CNG instead of fresh air causes the reduced turbulent flame propagation of ignition regions of the pilot fuel and as result higher amount of uHC is produced. Increasing the T_{in} and Φ led to higher gas temperature and as result, lower incomplete combustion, which means lower uHC emission. The final equations for uHC in terms of actual factors are given as Eqs. (2) and (3) below:

Engine speed 800 rpm

uHC=+12475:96-46436:12×A+1:53×B+189:75×A×B+15055:17×A2-0.3×B2 (2)

Engine speed 1500 rpm

uHC=+12103:77-46796.12×A+3:88×B+189:75×A×B+15055.17×A2-0.3×B2 (3)

3.3. CO emissions

Table 4 shows that all the considered factors (A, B and C) with the small p-values have significant influence on CO emissions under 99% confidence level. It should be noted that AB, AC and A^2 have p-value more than 0.05, and are thus not significant. Figure 6 exhibits the interaction effects of Φ and T_{in} on CO in different engine speeds. It can be concluded from the figures that by rising the Φ and T_{in}, CO diminishes for both 800 and 1500 rpm. Equally, from Figure 6, it is evident that amount of CO emissions decreases gradually with increase in T_{in} and Φ. The rate of CO formation is highly dependent on mixture temperature, the amount of available unburned fuel and control the rate of fuel decomposition and oxidation. So, for RCCI engines, the CO concentration is significantly higher than for CDC mode at all engine loads and speeds. In RCCI mode, fuel (CNG) and inducted air are mixed through the intake stroke of engine, leading to production of lower local fuel-rich region [6].

The reduced in-cylinder temperature in this mode, together with lower oxygen concentration, caused incomplete combustion and more CO and uHC. By increasing the T_{in}, the in-cylinder temperature will increase, and as result, the CO oxidation to CO_2 occurs easily. Also, by increasing the Φ, the load level of engine increases, lading to higher in-cylinder temperature (lower CO emission).

The following regression Eqs. (4) and (5) were developed by application of RSM to predict CO. These final quadratic equations are empirical

[DOI: 10.22068/ase.2020.533]

relationship between CO and the test variables, respectively, in terms of actual factors:

Engine speed 800 rpm

$$CO=+43654.37-45015.79\times A-362.17\times B+200.62\times A\times B+12251.72\times A^2+0.72\times B^2 \quad (4)$$

Engine speed 1500 rpm

$$CO=+43148.42-45765.79\times A-358.29\times B+200.62\times A\times B+12251.72\times A^2+0.72\times B^2 \quad (5)$$

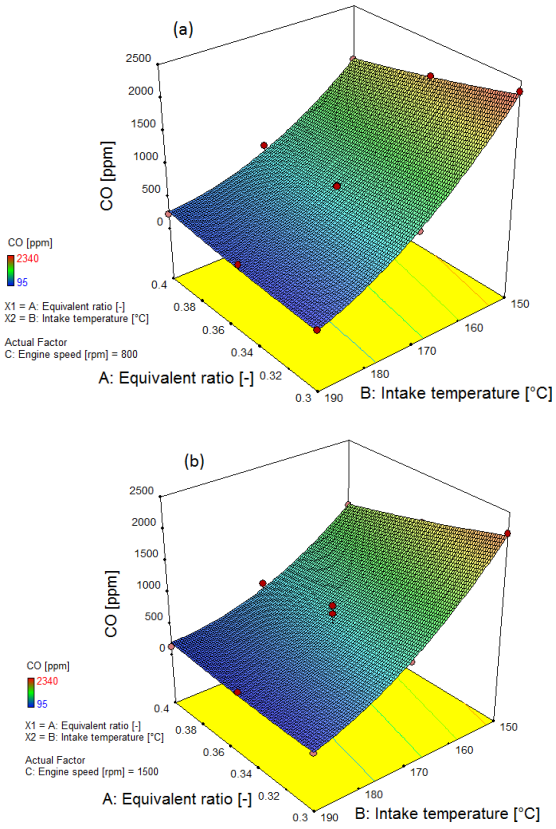

Figure 6: The interaction effects of Φ and T_{in} on the CO for two levels of engine speeds (a) 800 rpm and b) 1500 rpm)

3.4. NOx emissions

From ANOVA in Table 4, it can be inferred that Φ and T_{in}, followed by engine speed, have significant influence on NOx emissions. The interactive effect of Φ and T_{in} at all engine speeds on NOx emissions are shown in Figure 7. It can be seen that NOx emissions become low with reduction the amount of Φ and T_{in}. It can also be noted that NOx emission increases dramatically at higher amount of Φ and T_{in}. In this situation, the combustion temperature becomes higher with higher PPRR and promotes NOx formation. NOx formation in engine generally depends on oxygen concentration, incylinder temperature and available time for reactions. Higher Φ and T_{in} cause increased local temperatures and as result, the maximum temperature during combustion increases and leads to increased NOx formation . Table 4 shows that the values were fitted well to a quadratic model Eqs. (6) and (7), which describes NOx as a function of the Φ and T_{in}.

Engine speed 800 rpm

$$NOx=+13023.84-18261.73\times A-133.63\times B+174.87\times A\times B-11586.2\times A^2+0.25\times B^2 \quad (6)$$

Engine speed 1500 rpm

$$NOx=+12131:93-17115:07\_A-130.08\times B+174.87\times A\times B-11586.20\times A^2+0:25\times B^2 \quad (7)$$

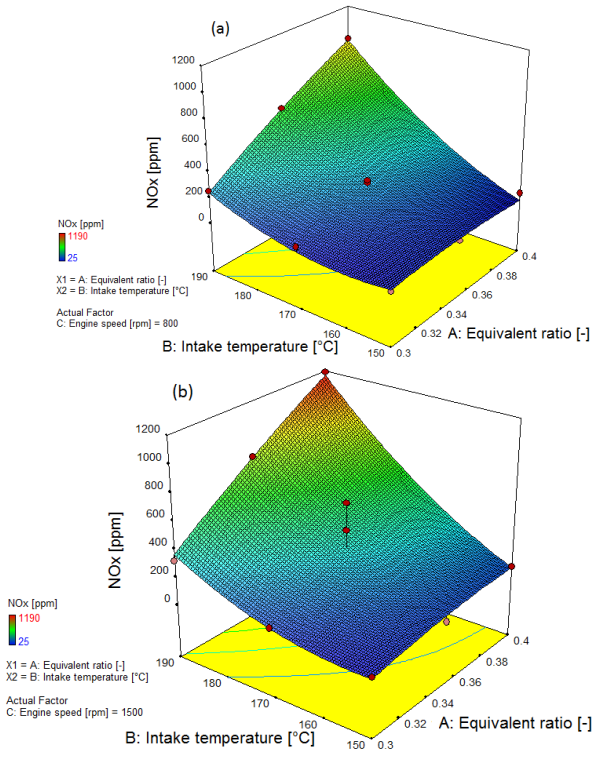

Figure 7: The interaction effects of Φ and T_{in} on the NOx for two levels of engine speeds (a) 800 rpm and b) 1500 rpm)

[DOI: 10.22068/ase.2020.533]

3.5. IMEP

As shown in Table 4, with comparison of the factors P-value, two parameters in the response surface quadratic model (B and C) are significant (P< 0:0001), which shows that T_{in} and engine speed are more effective on IMEP than Φ with less significant effect. The interactive effect of Φ and T_{in} on IMEP in various engine speed are shown in Figure 8. As shown, increasing of T_{in} along with raising the Φ resulted in the increase of IMEP. The second order polynomial equation of empirical data based on the actual factors is presented as Eqs. (8) and (9):

Engine speed 800 rpm

$$IMEP= +20:10-35.11\times A-0.07\_B-0.08\times A\times B+68.41\times A^2+4.25E-004\times B^2 \quad (8)$$

Engine speed 1500 rpm

$$IMEP= +13.23-21.40\times A-0.05\times B-0.08\times A\times B+68.41\times A^2+4.25E-004\times B^2 \quad (9)$$

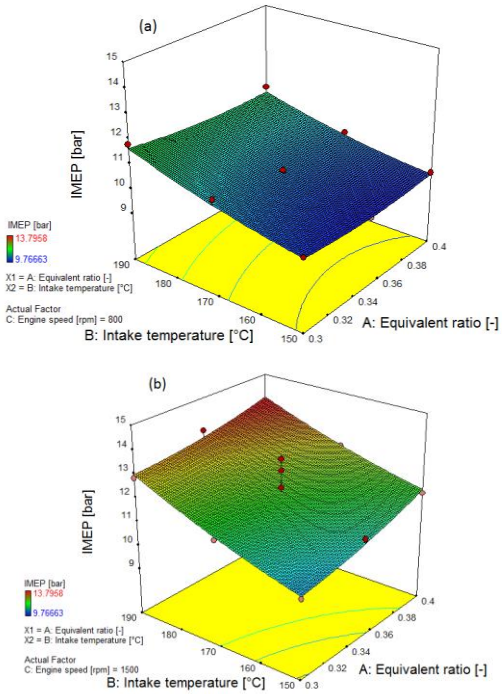

Figure 8: The interaction effects of Φ and T_{in} on the IMEP for two levels of engine speeds (a) 800 rpm and b) 1500 rpm)

3.6. CNL

The small p-values of all considered factors indicate that their contribution is not insignificant to CNL model as evidenced from ANOVA in Table 4 and there is a trade-off relation between Φ, T_{in}, engine speed and CNL. The model is significant in terms of closeness the values of R^2 and adjusted R^2 (Table 5). Figure 9 shows the interaction effects of Φ and T_{in} on CNL at different engine speed. These figures exhibit the increasing of CNL utilized by a rise in both the Φ and T_{in}. The response surface plot is almost flat at 800 rpm. The modification of Φ and T_{in} had little effect on CNL in this engine speed. In addition, higher amount of CNL were obtained for the RCCI experimental data at 1500 rpm. There is a sharp slope upwards when the Φ and T_{in} lead to the maximum.

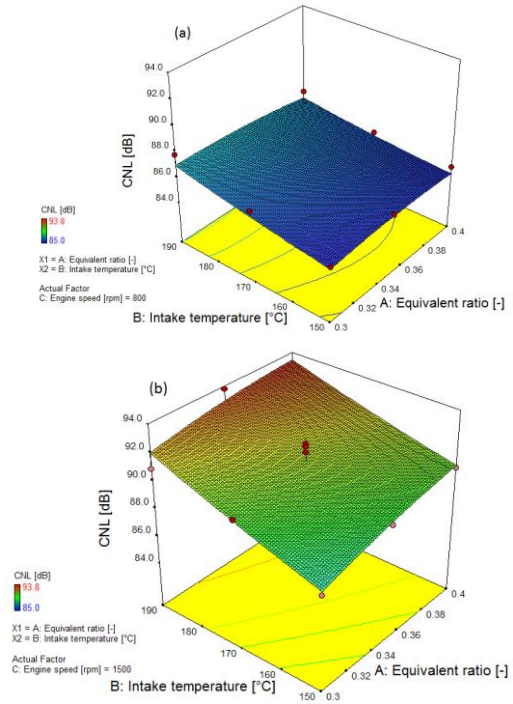

Figure 9: The interaction effects of Φ and T_{in} on the CNL for two levels of engine speeds (a) 800 rpm and b) 1500 rpm)

The second order polynomial model equation based on the actual factors for predicting CNL is presented as Eqs (10) and (11).

Engine speed 800 rpm

[DOI: 10.22068/ase.2020.533]

CNL= +65.05+98.21×A+4.32957E-003×B-0.20×A×B-92.98×A2+3.2E-004×B^2

(10)

Engine speed 1500 rpm

CNL= +54.61638+117.76×A+0.05×B-0.20×A×B-92.98×A^2+3.2E-004×B^2

(11)

3.7. Optimization

The criterion for optimization for the responses and their weights are presented in Table 6. The amount of optimized parameters and criteria of optimization for simultaneously satisfying the requirements placed on each of the responses (minimizing HC and CO, maximizing IMEP and keeping CNL in the range of 85-90 dB) were reported by the Design Expert software and presented in Table 7. In desirability based approach, at optimum input parameters, the values of uHC, CO, NOx, IMEP and CNL were found to be 90.3 (ppm), 106.8 (ppm), 248.2 (ppm), 11.7 (bar) and 87 (dB), respectively, with maximum desirability of 0.77.

Table 6: Optimization criteria of emissions, performance and combustion noise level.

Constraints name Limits	Target	Limits		Weight	
		Lower	Upper	Lower	Upper
uHC [ppm]	Minimize	70	1920	1	0.1
CO [ppm]	Minimize	95	2340	1	0.1
NOx [ppm]	Minimize	25	1190	1	0.1
IMEP [bar]	Maximize	9.76	13.79	0.1	1
CNL [dB]	In range	85	90	1	1

Table 7: Solutions from desirability approach closer to optimization criteria (uHC emissions: minimize, CO emissions: minimize, NOx emissions: minimize, IMEP maximize and CNL: in range)

T_{in} [◦C]	Φ [-]	N [rpm]	uHC [ppm]	CO [ppm]	NOx [ppm]	IMEP [bar]	CNL [dB]
190	0.3	800	90.3	106.8	248.2	11.7	87

3.8. Validation of optimization result

After performing the optimization, in order to validate the optimized results obtained using desirability approach, the experiment confirmation tests were performed at the optimal values of RCCI operational parameters. For the actual responses, the average of three measured results was calculated. Summary of the observed results of the confirmation tests (the average of experimentally calculated values), the predicted values and error percentage are shown in Table 9. The results indicate that the models developed using RSM for uHC, CO, NOx, IMEP and CNL were found to be adequate to describe the effect of the Φ and T_{in} on performance, combustion noise level and emissions for two levels of engine speeds. The model was validated by confirmatory tests, indicating the error in prediction less than 5% which are presented in Table 8.

Table 8: Validation of test results

T_{in} [◦C]	Φ [-]	N [rpm]		uHC [ppm]	CO [ppm]	NOx [ppm]	IMEP [bar]	CNL [dB]
190	0.3	800	Predicted	90.3	106.8	248.2	11.7	87
			Actual	88	112	259	12	87.9
			%Error	2.5	4.6	4.1	2.5	1.1

4. Summary and conclusions

An experimental and modeling study was carried out to analyze and predict uHC, CO, NOx, IMEP and CNL in RCCI engine. RSM-based models were developed for the first time in the literature to predict uHC, CO, NOx, IMEP and CNL in RCCI engine and the new method using RSM for RCCI engine testing was introduced to find operating points with minimum uHC, CO, NOx and maximum IMEP when combustion noise is not greater than 90 dB which prevents RCCI operation in the ringing region. Here is the list of the outcomes/findings from this study:

- RSM can be employed to develop models to predict uHC, CO, NOx, IMEP and CNL in RCCI engine. All the developed models

[DOI: 10.22068/ase.2020.533]

were found to be statistically significant because the p-values are less than 0.05.

- 3-D plots were developed using Design Expert (dx-7) software to show interactive effects of input factors on responses. The plots show that Φ and T_{in} have major influence on uHC and CO emissions. uHC and CO emissions were found to be low at higher Φ but NOx and IMEP are least at lowest Φ and T_{in}.
- The influence of Φ, T_{in} and engine speed were found to be maximum on CNL. CNL can be decreased with reducing Φ, T_{in} and engine speed. There is a sharp increase in CNL during higher Φ and T_{in} at 1500 rpm.
- The results of this study revealed that, at optimum input parameters, the values of uHC, CO, NOx, IMEP and CNL were found to be 90.3 (ppm), 106.8 (ppm), 248.2 (ppm), 11.7 (bar) and 87 (db), respectively which this operating point has the lowest amount of uHC, CO and NOx (emissions) with higher IMEP in the range of CNL between 85-90 dB which is not noisy operating point.
- Confirmation tests indicated that the developed RSM models were favorable and adequate for predicting uHC, CO, NOx, IMEP and CNL. The validation results by confirmatory tests show that the models can predict uHC, CO, NOx, IMEP and CNL with less than 5% error.

Acknowledgements

The authors would like to thank the thermodynamics laboratory of Amirkabir University of technology for providing the experimental facilities. We would also like to acknowledge the support provided by national elite foundation.

List of symbols (Optional)

Φ	equivalence ratio
aBDC	after bottom dead center
aTDC	after top dead center
AFR	air-fuel ratio
ANOVA	analysis of variance
BMEP	brake mean effective pressure
BP	brake power
BSFC	brake specific fuel consumption
BTE	brake thermal efficiency
BT	brake torque
CAD	crank angle degree
CCD	central composite design
CDC	conventional diesel combustion
CI	compression ignition
CNG	compressed natural gas
CNL	combustion noise level
CO	carbon monoxide
FFT	fast fourier transform
HCCI	homogeneous charge compression ignition
ICE	internal combustion engine
IMEP	indicated mean effective pressure
LTC	low temperature combustion
NG	natural gas
NOx	oxides of nitrogen
P_{filt}	filtered pressure
P_{RMS}	root mean square of filtered pressure
$P(\omega)$	in-cylinder pressure in frequency domain
PM	particulate matter
PPM	parts per million
PPR	pulses per revolution
PPRR	peak pressure rise rate
RI	ringing intensity
RCCI	reactivity control compression ignition
RMSE	root mean square error
RPM	revolution per minute
RSM	response surface method
T_{in}	intake temperature
TDC	top dead center
uHC	unburned hydrocarbon

References

[DOI: 10.22068/ase.2020.533]

[1] RD. Reitz, Directions in internal combustion engine research. Combust Flame, Vol.160, (2013), pp.1-8

[2] B. Bahri, AA. Aziz, M. Shahbakhti, MF. Muhamad Said, Understanding and detecting misfire in an HCCI engine fuelled with ethanol. Appl Energy, Vol.108, (2013), pp.24-33.

[3] J. Rezaie, M. Shahbakhti, B. Bahri, AA. Aziz, Performance prediction of HCCI engines with oxygenated fuels using artificial neural networks. Appl Energy, Vol.138, (2015), pp.460-73.

[4] M. Bidarvatan, V. Thakkar, M. Shahbakhti, B. Bahri, A. Abdul Aziz, Greybox modeling of HCCI engines. Appl Therm Eng, Vol.70, (2014), pp. 397-409.

[5] B. Bahri, AA. Aziz, M. Shahbakhti, MF. Muhamad Said, Ethanol fuelled HCCI engine: A review. Int J Mech Aero Indus Mech Manufac Eng, Vol.7, (2013), pp. 437-43.

[6] A. Gharehghani, R. Hosseini, M. Mirsalim, A. Jazayeri, T. Yusaf, An experimental study on reactivity controlled compression ignition engine fueled with biodiesel/natural gas. Energy, Vol.89, (2015), pp. 558-67.

[7] K. Poorghasemi, R. Khoshbakhti Saray, E. Ansari, B. Khoshbakht, M. Shahbakhti, JD. Naber, Effect of diesel injection strategies on natural gas/diesel RCCI combustion characteristics in a light-duty diesel engine. Appl Energy, Vol.199, (2018), pp. 430-46.

[8] M. Nazemi, M. Shahbakhti, Modeling and analysis of fuel injection parameters for combustion and performance of an RCCI engine. Appl Energy, Vol.165, (2016), pp. 135-50.

[9] S. Kokjohn, R. Hanson, D. Splitter, R. Reitz, Experiments and modeling of dual-fuel HCCI and PCCI combustion using in-cylinder fuel blending. AE Int J of Engines, Vol.2, (2010), pp. 24-39.

[10] S. Kokjohn, R. Hanson, D. Splitter, R. Reitz, Fuel reactivity controlled compression ignition (RCCI): a pathway to controlled high-efficiency clean combustion. Int J Engine Res, Vol.12, (2011), pp. 209-26.

[11] J. Benajes, A. Garc`ıa, JM. Pastor, J. Monsalve-Serrano, Effects of piston bowl geometry on Reactivity Controlled Compression Ignition heat transfer and combustion losses at different engine loads. Energy, Vol.98, (2016), pp. 64-77.

[12] L. Zhu, Y. Qian, X. Wang, X. Lu, Effects of direct injection timing and premixed ratio on combustion and emissions characteristics of RCCI (Reactivity Controlled Compression Ignition) with N-heptane/gasoline-like fuels. Energy Vol.93, (2015), pp. 383-92.

[13] B. Rajesh Kumar, S. Saravanan, D. Rana, A. Nagendran, Combined effect of injection timing and exhaust gas recirculation (EGR) on performance and emissions of a DI diesel engine fuelled with next-generation advanced biofuel-diesel blends using response surface methodology. Energy Convers Manage, Vol.123, (2016), pp. 470-86.

[14] S. Saravanan, B. Rajesh Kumar, A. Varadharajan, D. Rana, B. Sethuramasamyraja, G. Lakshmi Narayana rao, Optimization of DI diesel engine parameters fueled with iso-butanol/diesel blends-Response surface methodology approach. Fuel, Vol.203, (2017), pp. 658-70.

[15] DT. Montgomery, RD. Reitz, Optimization of heavy-duty diesel engine operating parameters using a response surface method. SAE Paper No. 2000-01-1962; 2000.

[16] T. Ganapathy, RP. Gakkhar, K. Murugesan, Optimization of performance parameters of diesel engine with Jatropha biodiesel using response surface methodology. Int J Sustain Energ, Vol.30, (2011), pp. 76-90.

[17] JB. Hirkude, AS. Padalkar, Performance optimization of CI engine fuelled with waste

[DOI: 10.22068/ase.2020.533]

fried oil methyl ester-diesel blend using response surface methodology. Fuel, Vol.119, (2014), pp. 266-73.

[18] S. Dhingra, G. Bhushan, KK. Dubey, Performance and emission parameters optimization of mahua (Madhuca indica) based biodiesel in direct injection diesel engine using response surface methodology. J Renew Sustain Energy, Vol.5, (2013), pp. 10-20.

[19] A. Atmanli, B. Y ¨ uksel, E. Ileri, A. DenizKaraoglan, Response surface methodology based optimization of dieseln-butanol cotton oil ternary blend ratios to improve engine performance and exhaust emission characteristics. Energy Convers Manage, Vol.90, (2015), pp. 383-94.

[20] E. Ileri, AD. Karaoglan, A. Atmanli, Response surface methodology based prediction of engine performance and exhaust emissions of a diesel engine fuelled with canola oil methyl ester. J Renew Sustain Energy, Vol.5, (2013), pp. 24-30.

[21] Z. Win, RP. Gakkhar, SC. Jain, M. Bhattacharya, Parameter optimization of a diesel engine to reduce noise, fuel consumption, and exhaust emissions using response surface methodology. Proc Inst Mech Eng, Part D: J Automobile Eng, Vol.219, (2005), pp. 1181-92.

[22] G. Najafi, B. Ghobadian, T. Yusaf, SM. Ardebili, Safieddin, R. Mamat, Optimization of performance and exhaust emission parameters of a SI (spark ignition) engine with gasolineethanol blended fuels using response surface methodology. Energy, Vol.90, (2015), pp. 1815-29.

[23] OI. Awad, R. Mamat, OM. Ali, WH. Azmi, K. Kadirgama, IM. Yusri et al., Response surface methodology (RSM) based multi-objective optimization of fusel oil-gasoline blends at different water content in SI engine. Energy, Vol.150, (2017), pp. 222-41.

[24] IM. Yusri, R. Mamat, WH. Azmi, AI. Omar, MA. Obed, AIM. Shaiful, Application of response surface methodology in optimization of performance and exhaust emissions of secondary butyl alcohol-gasoline blends in SI engine. Energy Convers Manage, Vol.133, (2017), pp. 178-95.

[25] W. Fang, D. Kittelso, WF. Northrop, Optimization of reactivitycontrolled compression ignition combustion fueled with diesel and hydrous ethanol using response surface methodology. Fuel, Vol.160, (2019), pp. 446-457.

[26] A. Shahlari, C. Hockin, E. Kurtz, J. Ghandhi, Comparison of compression ignition engine noise metrics in low-temperature combustion regimes. SAE Int J Engines, Vol.6, (2013), pp. 541-52.

[27] B. Bahri, M. Shahbakhti, AA. Aziz, Real time modeling of ringing in HCCI Engines using artificial neural network. Energy 2017;125:509-18.

[DOI: 10.22068/ase.2020.533]